

AFWL-TR-81-24

AFWL-TR-81-24

AD A106348

HSURIA CONE CENTRATION

C. R. DeHainaut
E. L. Coates

September 1981



Final Report

S DTIC
ELECTE
OCT 30 1981
A

Approved for public release; distribution unlimited.

FILE COPY

AIR FORCE WEAPONS LABORATORY
Air Force Systems Command
Kirtland Air Force Base, NM 87117

0110300

AFWL-TR-81-24

This final report was prepared by the Air Force Weapons Laboratory, Kirtland Air Force Base, New Mexico, under Job Order 317J0796. Mr C. R. DeHainaut (ARAA) was the Laboratory Project Officer-in-Charge.

When US Government drawings, specifications, or other data are used for any purpose other than a definitely related Government procurement operation, the Government thereby incurs no responsibility nor any obligation whatsoever, and the fact that the Government may have formulated, furnished, or in any way supplied the said drawings, specifications, or other data, is not to be regarded by implication or otherwise, as in any manner licensing the holder or any other person or corporation, or conveying any rights or permission to manufacture, use, or sell any patented invention that may in any way be related thereto.

This report has been authored by an employee of the United States Government. Accordingly, the United States Government retains a nonexclusive, royalty-free license to publish or reproduce the material contained herein, or allow others to do so, for the United States Government purposes.

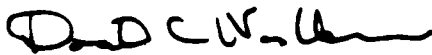
This report has been reviewed by the Public Affairs Office and is releasable to the National Technical Information Service (NTIS). At NTIS, it will be available to the general public, including foreign nations.

This technical report has been reviewed and is approved for publication.



C. R. DEHAINAUT
Project Officer

FOR THE COMMANDER



DONALD C. WASHBURN
Lt Colonel, USAF
Chief, Advanced Beam Control Branch



DAVID W. SEEGMILLER
Colonel, USAF
Chief, Advanced Laser Tech Division

DO NOT RETURN THIS COPY. RETAIN OR DESTROY.

UNCLASSIFIED

SECURITY CLASSIFICATION OF THIS PAGE (When Data Entered)

REPORT DOCUMENTATION PAGE		READ INSTRUCTIONS REPORT COMPLETION FORM
1. REPORT NUMBER APML-TR-81-24	2. GOVT ACCESSION NO. 21 APR 82	3. RECIPIENT CATALOG NUMBER
4. TITLE (and Subtitle) HSURIA CONE CENTRATION	5. TYPE OF REPORT & PERIOD COVERED Final Report	
6. AUTHOR(s) C. R. DeMainaut E. L. Coates	7. PERFORMING ORG. REPORT NUMBER	
8. PERFORMING ORGANIZATION NAME AND ADDRESS Air Force Weapons Laboratory (ARAA) Kirtland Air Force Base, NM 87117	9. CONTRACT OR GRANT NUMBER(s)	
11. CONTROLLING OFFICE NAME AND ADDRESS Air Force Weapons Laboratory (ARAA) Kirtland Air Force Base, NM 87117	10. PROGRAM ELEMENT PROJECT TASK AREA & WORK UNIT NUMBERS 626180/317J0796	
14. MONITORING AGENCY NAME & ADDRESS (if different from Controlling Office)	12. REPORT DATE September 1981	
	13. NUMBER OF PAGES 40	
16. DISTRIBUTION STATEMENT (of this Report) Approved for public release; distribution unlimited.	15. SECURITY CLASS. (of this report) Unclassified	
	15a. DECLASSIFICATION DOWNGRADING SCHEDULE	
17. DISTRIBUTION STATEMENT (of the abstract entered in Block 20, if different from Report)		
18. SUPPLEMENTARY NOTES		
19. KEY WORDS (Continue on reverse side if necessary and identify by block number) Unstable Resonators Laser Cavities-----Structure Laser Cavities-----Alignment		
20. ABSTRACT (Continue on reverse side if necessary and identify by block number) A technique for alignment of the rear cone in a half symmetrical unstable resonator with internal axicons (HSURIA) is discussed. Special hardware built to test this technique is described, and test results are analyzed.		

DD FORM 1 JAN 73 1473

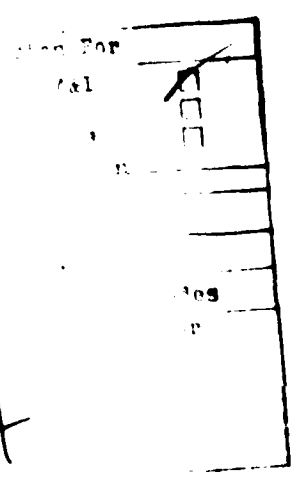
UNCLASSIFIED

SECURITY CLASSIFICATION OF THIS PAGE (When Data Entered)

0132

CONTENTS

<u>Section</u>		<u>Page</u>
I	INTRODUCTION	3
II	BACKGROUND	5
III	THEORY OF OPERATION	6
	1. EFFECT OF CONE DECENTRATION	6
	2. THE CONE CENTRATION SENSOR	6
IV	TEST CONFIGURATION	14
	1. GENERAL LAYOUT	14
	2. LENS-RETICLE ASSEMBLY	16
	3. LATERAL CELL POSITION SENSOR ASSEMBLY	16
	4. MIRROR POSITIONING HARDWARE	16
	5. SPIDER MIRROR MOUNT	22
V	ELECTRONICS	23
	1. AEROTECH ELECTRONICS	23
	2. ROTATING DETECTOR AMPLIFIER	23
	3. DIVIDE CIRCUIT	26
	4. LOCK-IN AMPLIFIER	26
	5. CONTROL AND DISPLAY PANEL	29
	6. THE DETECTOR	29
VI	ALIGNMENT OF OPTICS	30
	1. OVERALL ALIGNMENT	30
	2. ROTATING SENSOR TO CONE ALIGNMENT	30
	3. LENS TO WAXICON TIP ALIGNMENT	31
VII	EFFECT OF MISALIGNMENTS ON CENTRATION SENSOR ACCURACY	32
	1. LASER ALIGNMENT	32
	2. WAXICON ALIGNMENT	32
	3. LENS ALIGNMENT	33
	4. SPIDER MIRROR ALIGNMENT	34
	5. SENSOR ALIGNMENT	34
VIII	ERROR SOURCES	35
	1. STATIC ERROR	35
	2. DYNAMIC ERROR	35



AFWL-TR-81-24

CONTENTS (Continued)

<u>Section</u>		<u>Page</u>
IX	TEST RESULTS	38
	1. PERFORMANCE	38
	2. PERFORMANCE OF THE SIMPLIFIED SYSTEM	38
X	CONCLUSION	40

I. INTRODUCTION

The half symmetric unstable resonator with internal axicons (HSURIA) is a promising concept for high-power lasers because it can take advantage of an annular gain region. The alignment of the optical elements in a HSURIA is critical to the laser's performance, but for certain configurations, such a fine alignment is difficult to achieve with conventional alignment methods.

In a reflexicon HSURIA (Fig. 1), after the reflexicon has been internally aligned, both the reflexicon and the cone must be centered to the optical axis of the system. The presence of the gain generator and the center portion of the reflexicon precludes alignment by sighting down the optical axis of the system to cross hairs mounted at the center of the cone. Interferograms of the resonator provide little information about the alignment of the cone. However, a centration sensor can produce a direct reading of cone misalignment despite these constraints.

This report describes a centration sensor system which measures the centration of the cone. The theory behind the sensor system and its construction are explained. The experimental procedures used to evaluate the sensor system's performance are described. Sources of error are identified and quantified.

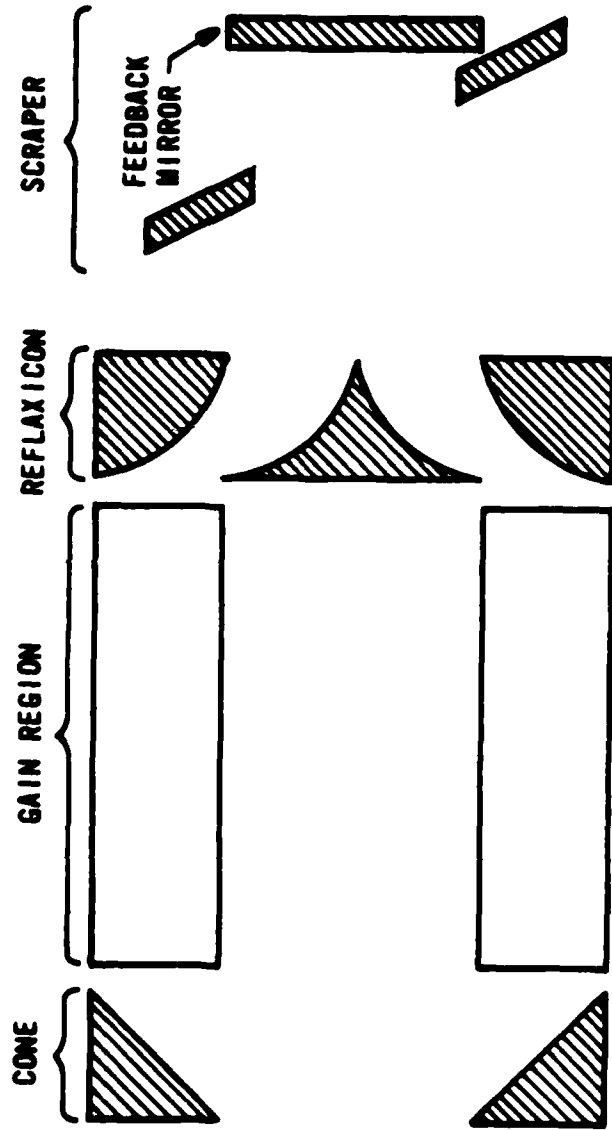


Figure 1. Reflaxicon HSURIA resonator.

II. BACKGROUND

The concept behind the alignment system described in this report was first published by Graham Flint (Ref. 1) of International Laser Systems in 1978. The concept was elaborated on by David M. Swain (Ref. 2). The design, construction, and testing described herein were performed by the Air Force Weapons Laboratory (AFWL).

1. Flint, Graham, "Notes on the Alignment of Annular Resonator Optics," International Laser Systems R&D Contract Status Report for the period ending 30 November 1978, Contract F29601-77-C-0048, p. 21.
2. Swain, David M., "Centration of a Linear Cone to the Optical Axis of a Reflexicon," Proceedings of the Society of Photo-Optical Instrumentation Engineers, Vol. 251, p. 131, July 1980.

III. THEORY OF OPERATION

Proper operation of an annular resonator (Fig. 1) requires that the cone be aligned with the optical axis of the resonator in both angle and centration. This ensures that the annular beam impinging on the cone is superimposed upon itself on reflection. The LS-14 laser error budget allows only 150 μm error in cone centration and 25 μrad error in cone tilt.

1. EFFECT OF CONE DECENTRATION

Decentration of the cone with respect to the optical axis of the resonator (Fig. 2) produces a translation in the beam reflected from the cone (Fig. 3). The reflected beam remains parallel to the optical axis, and no optical path differences (OPDs) are produced. (An ACCOS ray trace confirmed this.) The compacted returning beam is no longer superimposed on the impinging beam because of the translation. This effect was observed with the setup shown in Figure 4. Figure 5 shows the return beam with the cone centered and off center 1 mm, 2 mm, and 4 mm. The dark spots labeled 1 and 2 in Figure 5 are caused by a single small blemish on the inner surface of the waxicon beam compactor. The dark spot labeled 3 is caused by rounding of the tip of the waxicon. The change in the return beam can most easily be identified by observing the shadows of the spider mirror struts (Fig. 5). The cone was centered to an accuracy of ± 1 mm by observing these shadows.

Figure 6 shows interferograms taken with the setup shown in Figure 4. Slight differences between the fringe patterns are due to aberrations in the waxicon and cone. These interferograms do not contain any information about the alignment of the rear cone which is not contained in the return images (Fig. 5).

2. THE CONE CENTRATION SENSOR

A centration sensor has been built which measures the centration of the cone without relying on interferometry.

The centration sensor (Fig. 7) includes a collimated laser source and a weak positive lens which focuses the beam to a point at the center of the cone. As the annular beam from the waxicon approaches the cone, the annulus becomes very narrow. Assume that the annulus is reduced to two parallel rays striking opposite sides of the cone. The cone and waxicon axes are collinear

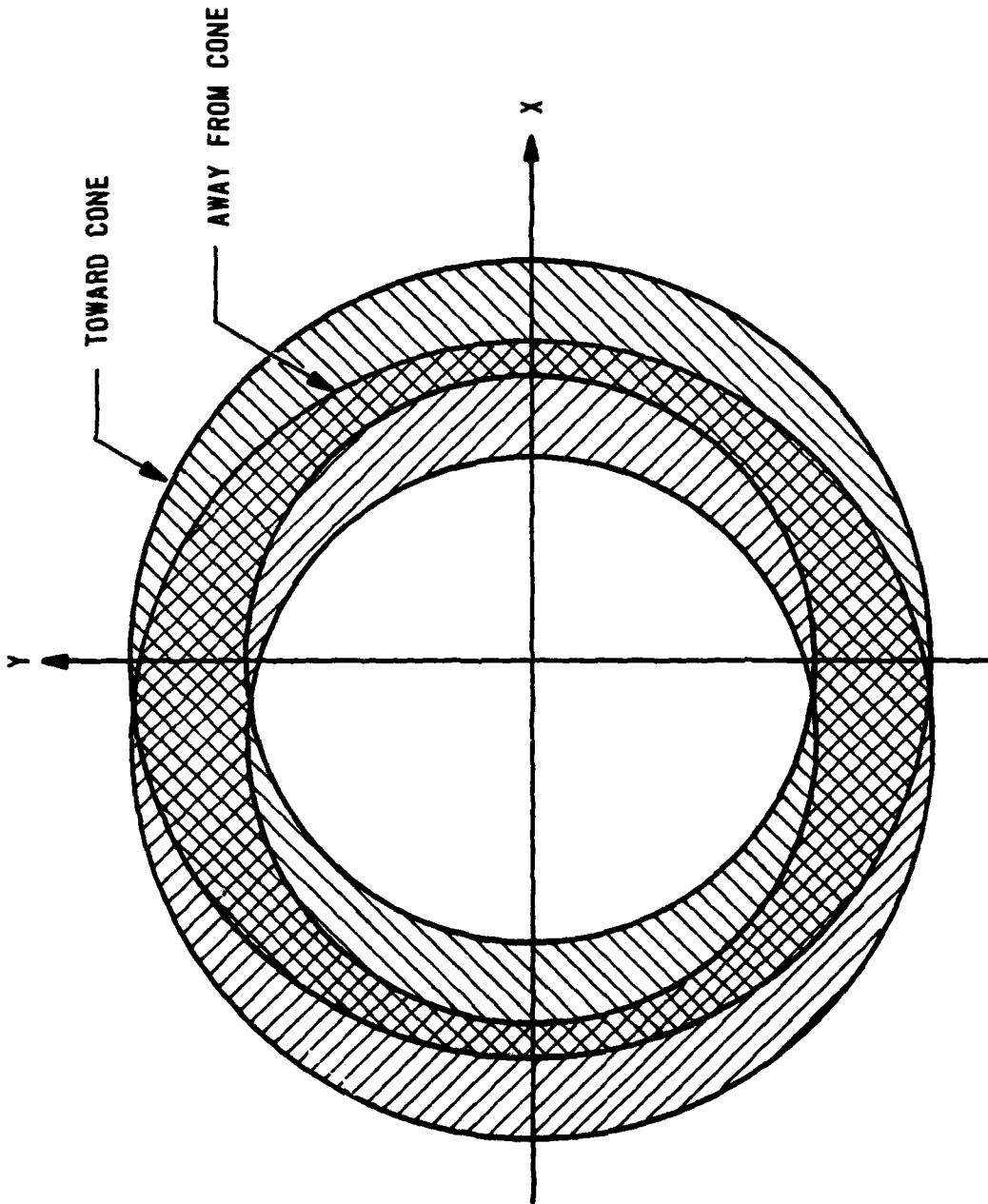


Figure 2. Effect of cone misalignment.

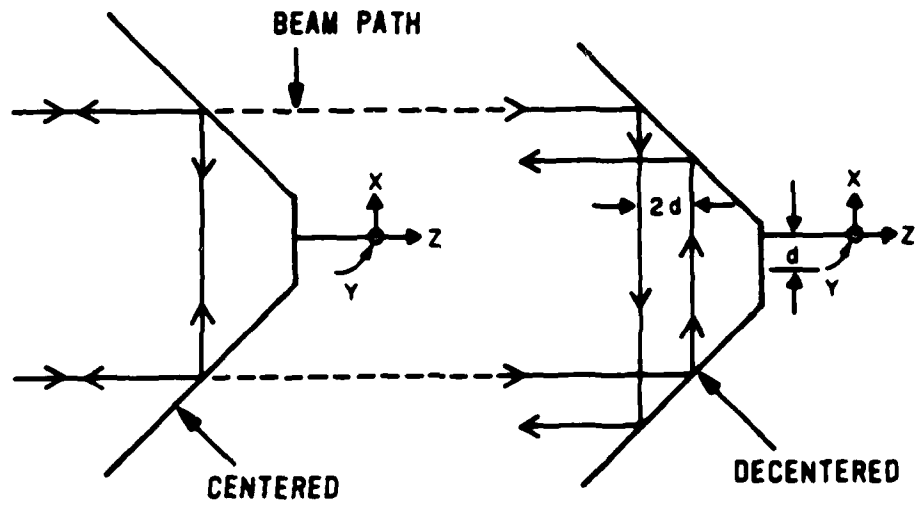


Figure 3. Cone aligned in angle, but decentered.

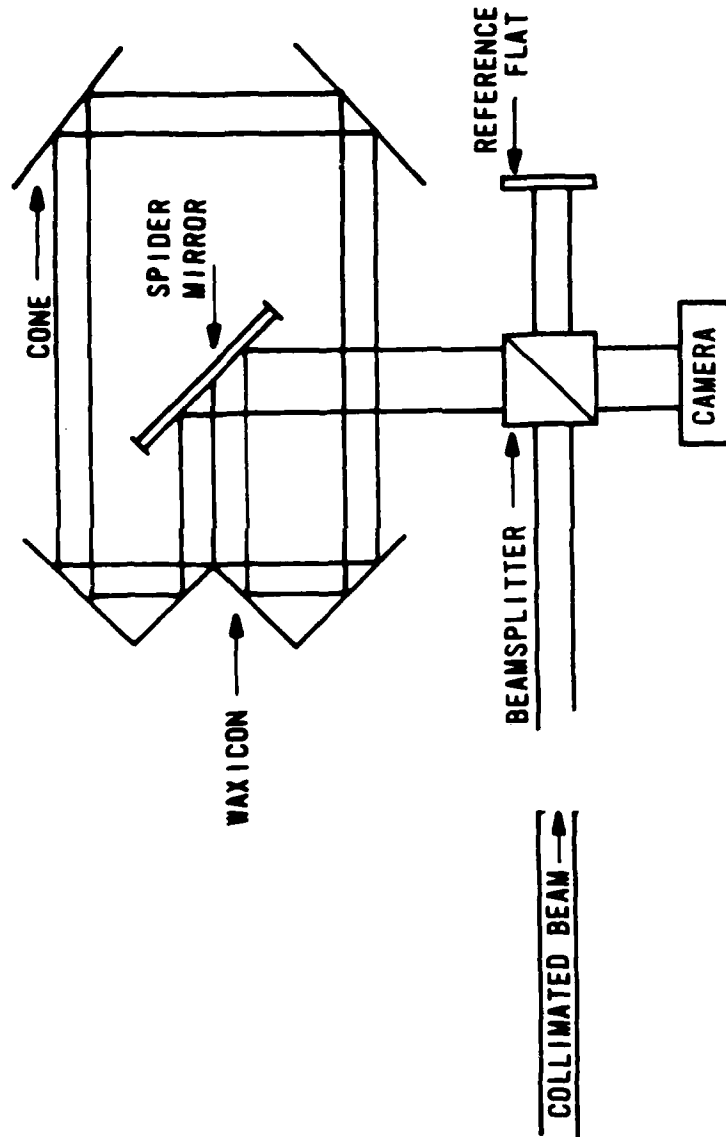
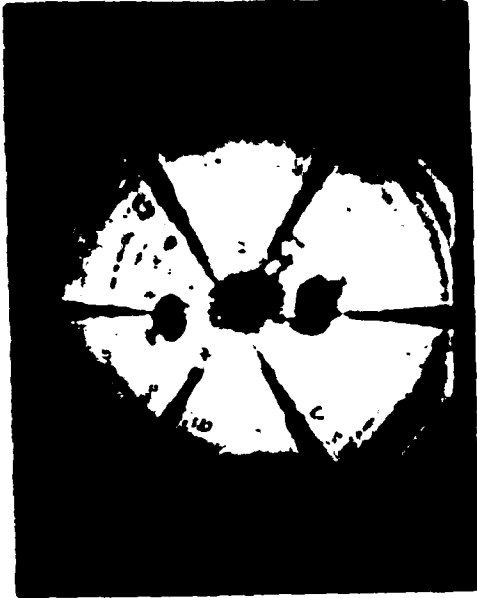


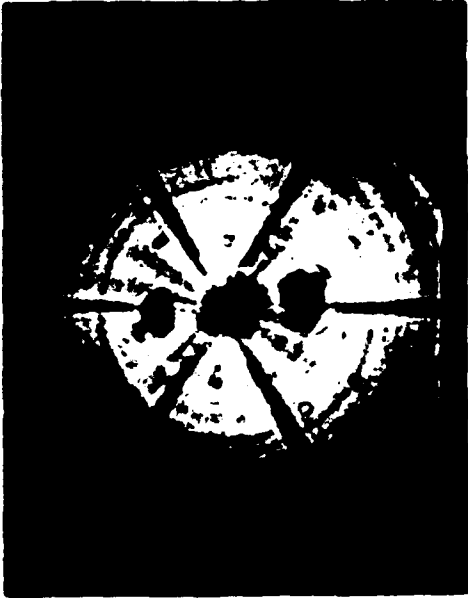
Figure 4. Optical setup, interferometer configuration.



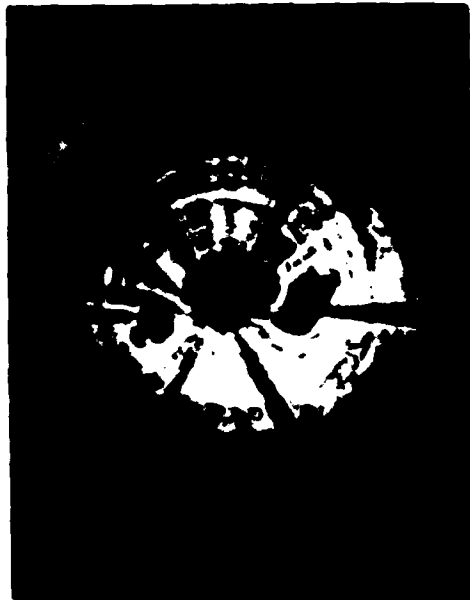
(b) Decentered 1 mm.



(d) Decentered 4 mm.



(a) Centered.

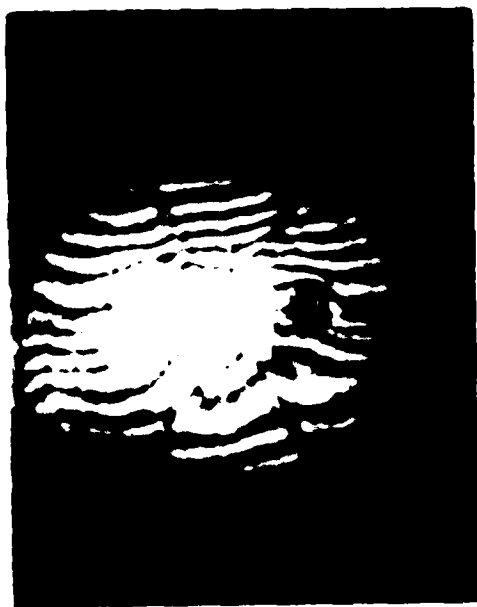


(c) Decentered 2 mm.

Figure 5. Return image, for various decenterations, of the rear one



(a) Centered.



(b) Decentered 2 mm.



(c) Decentered 4 mm.



(d) Decentered 2 mm.

Figure 6. Interferograms for various decentrations of the rear lens.

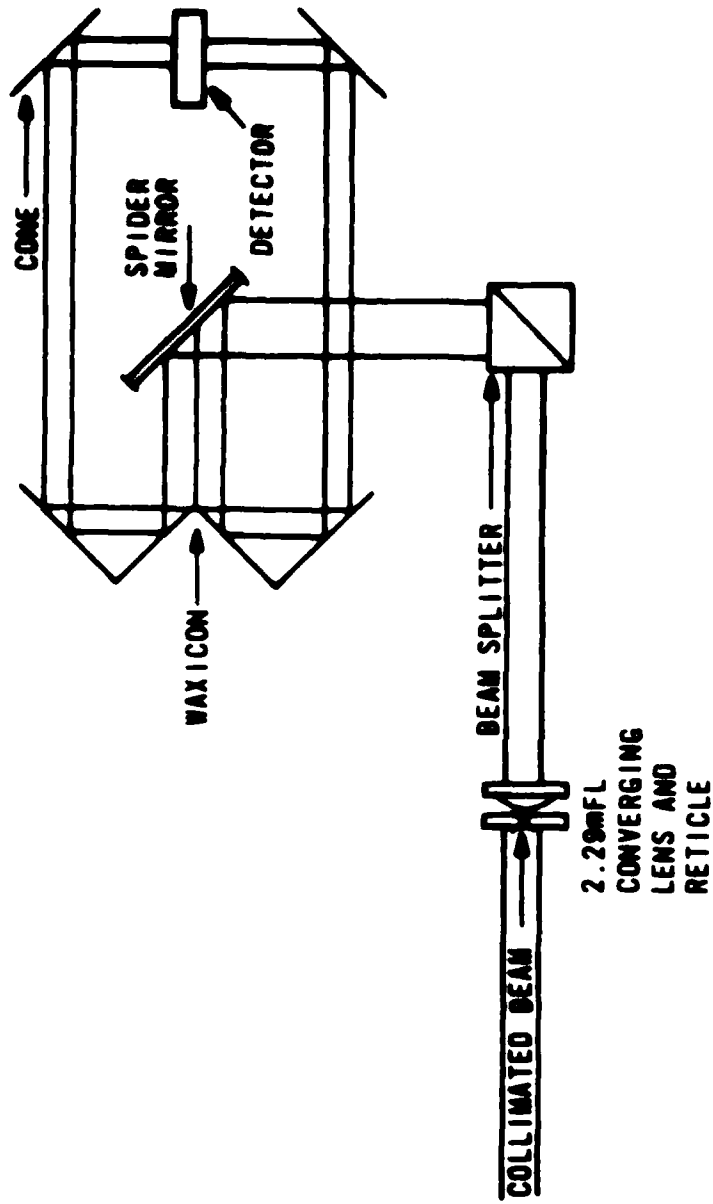


Figure 7. Optical setup, concentration sensor configuration.

with the Z axis. The rays are parallel to it. Each ray strikes the cone and is reflected to the point where the other ray struck the cone and then each is reflected once again, away from the cone each along the approach path of the other. That is, the rays exchange paths so that the reflection path of each is superimposed upon approach path of the other (Fig. 3). If the cone is decentered by distance d along the X axis, the rays are no longer superimposed but are displaced by $2d$ where they cross the Z axis and exit from the cone as shown by Figure 3. They are still parallel. Also, the input and output beams still coincide in the Y and Z planes because there is no misalignment there. When the sensor mounted position detector in the cone is rotated, it picks up the $2d$ displacement across the Z axis and registers the amplitude of the position change. This amplitude is the magnitude of the decentration. The phase of the position change with respect to the detector angle gives the direction of the decentration.

The centration sensor is insensitive to cone tilt. Assume that, as illustrated in Figure 8, the cone is centered, but tilted slightly about its apex. The upper and lower beams still pass the axis of the cone at the same point, so the centration sensor does not see any of the tilt error. In the laboratory, the centration sensor sometimes appears to be sensitive to cone tilt because the cone tilt adjustments rotate the cone about a point other than the cone's apex, but in fact, it is not.

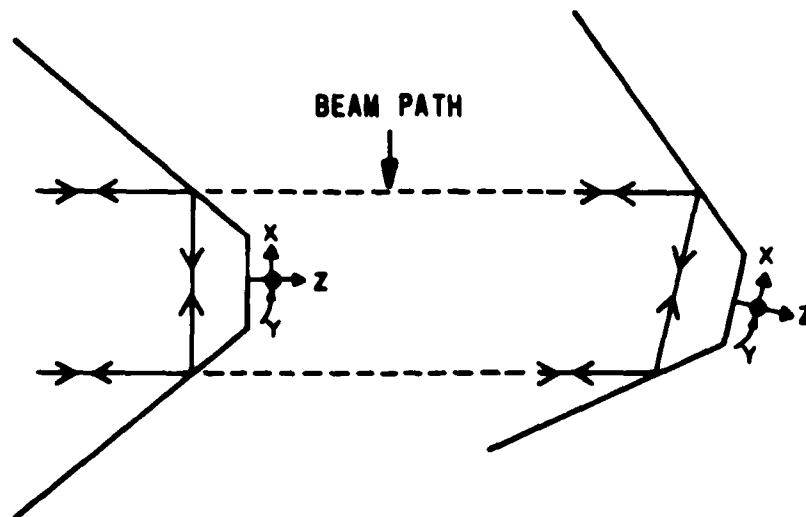


Figure 8. Cone centered, but misaligned in angle.

IV. TEST CONFIGURATION

1. GENERAL LAYOUT

The tests were conducted using a waxicon because a reflaxicon was not available. The results are applicable to either waxicon or reflaxicon systems. Two slightly different optical configurations were used--the centration sensor configuration shown schematically in Figure 7 and the interferometric configuration shown schematically in Figure 4.

a. Centration sensor configuration. As is shown in Figure 7, a collimated beam of light is focussed by the converging lens and passes into the resonator, eventually reaching the detector. As the detector is rotated along the Z axis of the cone, any misalignment of the cone will cause the Z-axis position of the beam on the detector to vary. The position information gathered by the detector when processed (see Section V-4) yields the decentration of the cone. The position and angle of the cone are monitored during the tests by Kaman probes and by an electronic autocollimator as shown in Figure 9. In an actual high-power laser, the centration sensor would have to be removed before firing the laser.

b. Interferometer configuration. This configuration (Fig. 4) uses a Twyman-Green interferometer to measure the cone centration for comparison with the results from the rotating detector configuration. The position and angle of the cone are again monitored by Kaman probes and an electronic autocollimator. The interferometer mode, as was explained in Section III-1, gave very little information about the alignment of the cone.

c. Physical layout. Figure 9 is a scale diagram of the equipment layout showing the arrangement for both test configurations. For the centration sensor configuration, the camera turning flat (5) must be removed and the centration sensor laser is used. The interferometer laser is turned off. For the interferometer configuration, the camera turning flat is replaced, the detector spindle is removed, and the interferometer laser is used. The centration sensor laser is turned off.

The change from one configuration to the other does not affect the optical alignment of the overall setup. This was because the detector spindle can be easily removed and replaced with an accuracy of 50 μm and

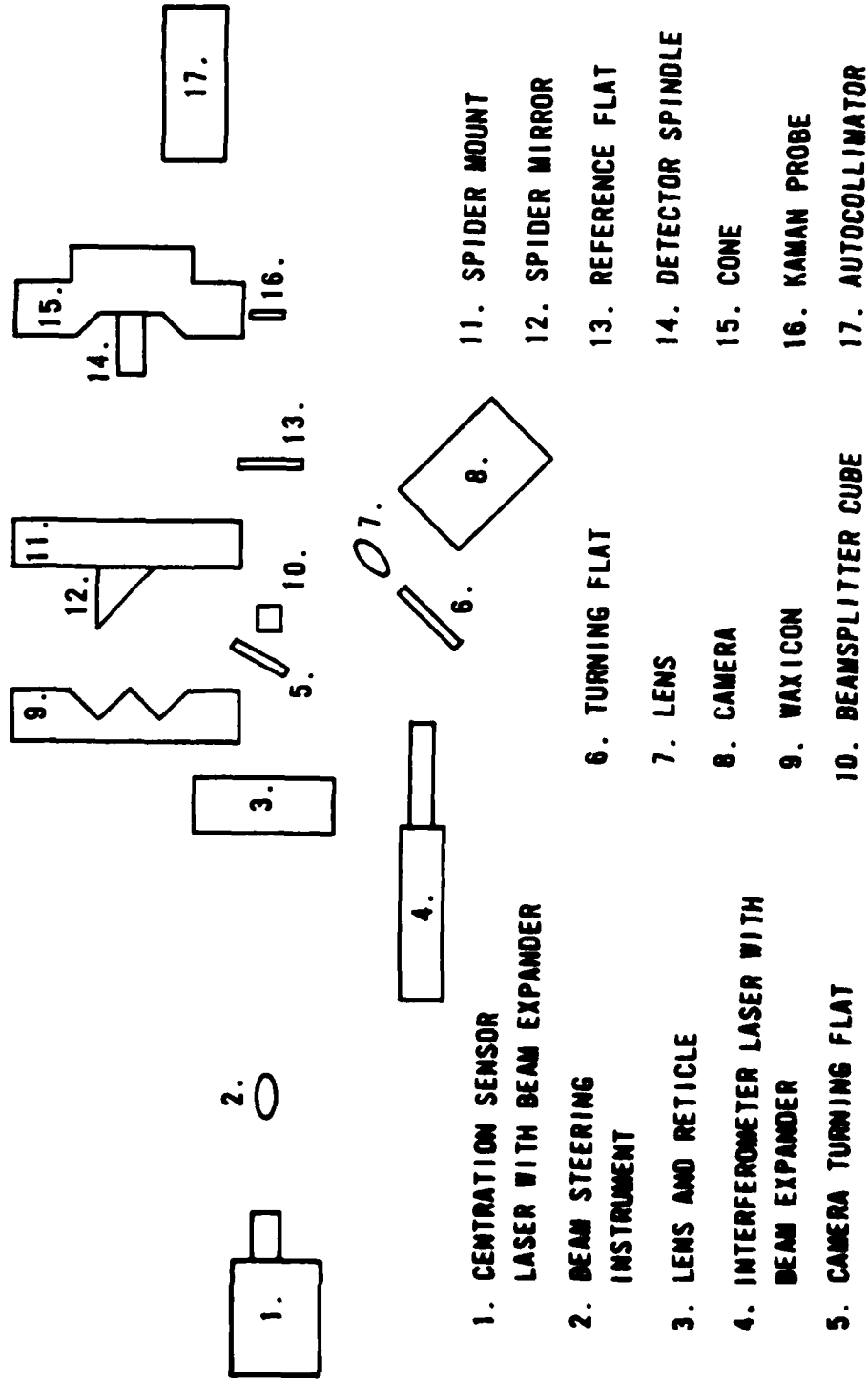


Figure 9. Diagram of experiment layout.

because the alignment of the camera turning flat affects only the position of the image in the camera and, therefore, is not critical.

2. LENS-RETICLE ASSEMBLY

The lens-reticle assembly, shown in Figure 10, was constructed by International Laser Systems, Inc. (ILS). It consists of a 6-in diameter f-50 doublet with a 21-mm reticle mounted together in a rotating mount with provision for independent centering of the lens and the reticle. The rotating mount is supported by precision bearings and rotated by a small motor. The whole assembly mounts in a 9-in Aerotech mirror mount. The use of the rotation to align the reticle to the center of the lens and the accuracies achieved are described in Section VI-3. Once aligned to the lens, the reticle was used to align the laser beam to the waxicon.

3. LATERAL CELL POSITION SENSOR ASSEMBLY

The lateral cell position sensor mount, or spindle, (Fig. 11) mounted the lateral cell position detector (Fig. 12) to the detector rotator (Fig. 13), and performed other important functions. One of these was providing for translation of the sensor along the axis of rotation to accommodate various sized beams at the waxicon by means of slotted holes in the detector mounting board. Another function was to allow accurate alignment of the sensor surface to the axis of rotation of the assembly through shimming of either the printed circuit board or the position sensor. The 1-in mirror on the front of the spindle monitored the alignment of the rotator to the cone as described in Section VI-2. An aperture which limits the sensor field of view to 20 deg was mounted on the spindle. The use of these alignment provisions is explained in Section VI-2.

4. MIRROR POSITIONING HARDWARE

The mirror positioning hardware permitted accurate positioning of the waxicon, cone, and spider mirror in azimuth, elevation, X translation (perpendicular to the optical axis and parallel to the table), and Y translation (height). This setup is illustrated in Figure 14. The 12-in Aerotech mount has a resolution of 3 μ rad per division on the micrometer in azimuth and elevation. The Klinger translation stages have a resolution of 5 μ m per division on the micrometer.

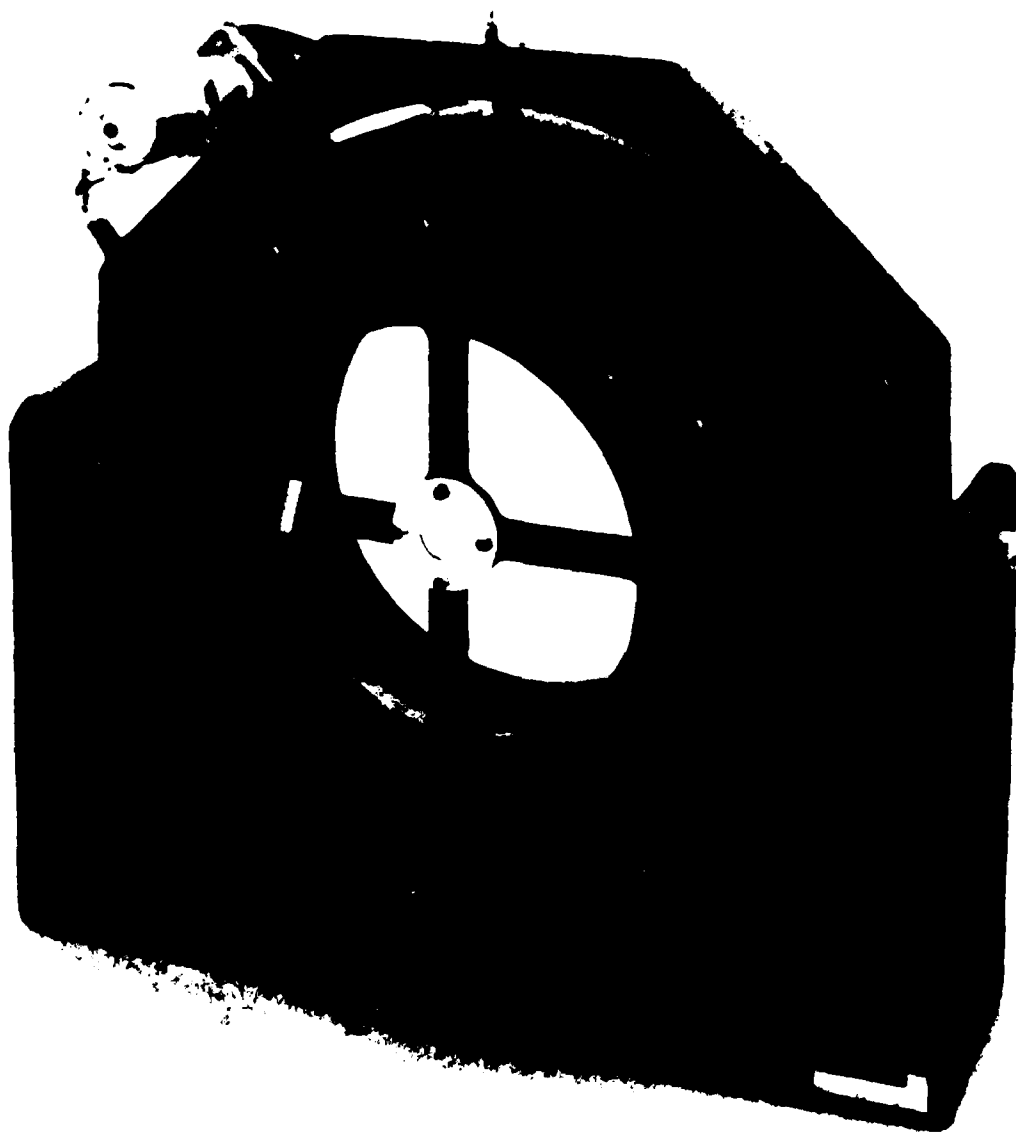
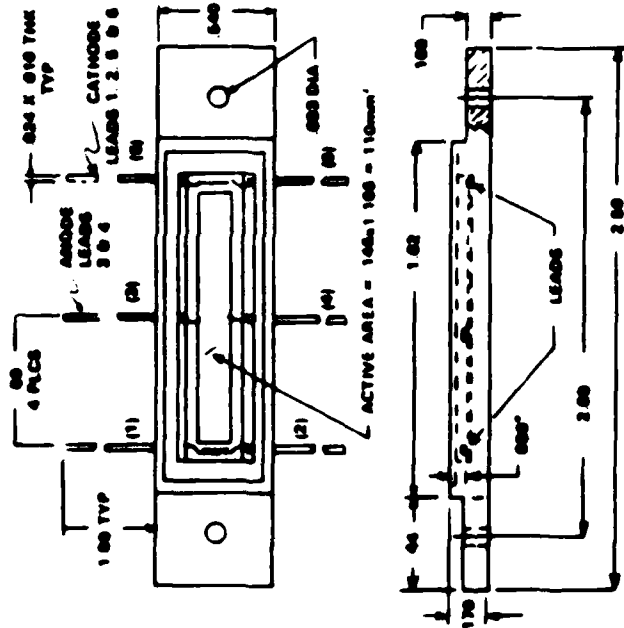


Figure 10. Lens - Reticle assembly.



Figure 11. Lateral cell position sensor mount.



* DIMENSION FROM OUTSIDE OF WINDOW TO ACTIVE AREA OF PHOTOHODE

Figure 12. Lateral cell position detector.

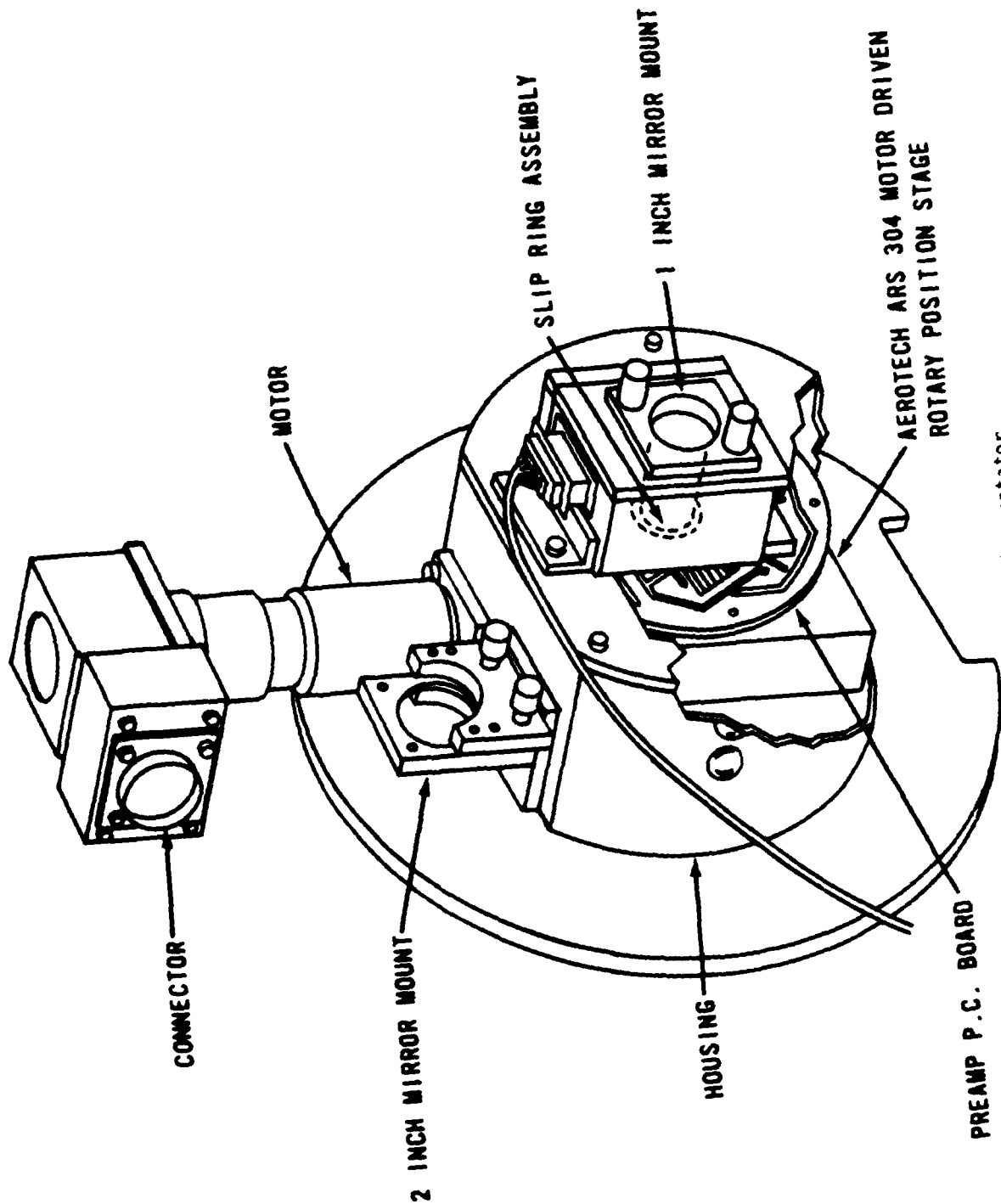


Figure 13. Detector rotator.

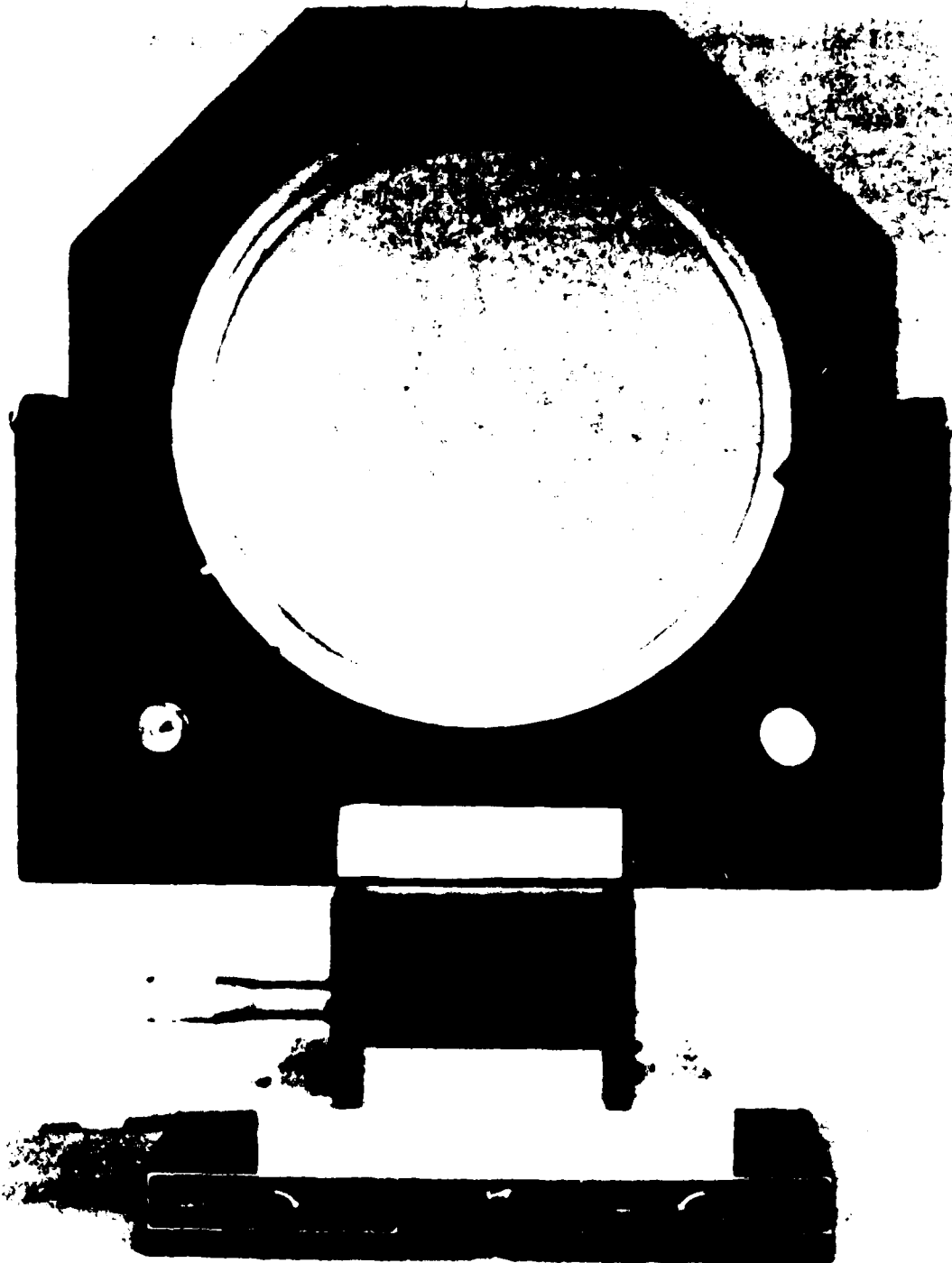


Figure 14. Mirror positioning hardware.

5. SPIDER MIRROR MOUNT

The spider mirror mount holds an elliptical flat mirror at a 45-deg angle in the center of a 12-in Aerotech mirror mount. The mirror is supported by six equally spaced struts 0.218 in thick. The mirror can be rotated about the Z-axis by loosening the mounting screws, rotating the mirror assembly, then tightening the screws. Fine adjustments to the mirror's angle are made with the adjustments on the Aerotech mount.

V. ELECTRONICS

The electronics continuously process the information received from the detector, providing an update on cone X and Y centration errors once during each detector revolution. The detector rotates at a constant speed ranging from 0.1 r/s to 1 r/s, the maximum speed of the rotation stage. The decentration is displayed on two meters on the control and display panel and is also sent to the instrumentation systems. The overall electronics block diagram is shown in Figure 15. The electronics subsystems are described below.

1. AEROTECH ELECTRONICS

The detector spindle was mounted on an Aerotech ARS-304 rotator powered by a DC motor. A modified Aerotech DC motor controller used feedback from a tachometer to keep the rotation speed constant as required by the lock-in amplifier.

2. ROTATING DETECTOR AMPLIFIER

The detector amplifier (Fig. 16) is built on a circular printed circuit (PC) board which rotates along with the lateral cell position detector. The preamp PC board is located as shown in Figure 13. It processes the signals from the detector and amplifies them to a level where they may be transmitted (with minimum noise) through the slip ring assembly to the nonrotating part of the system.

The amplifier produces two outputs. The first is the sum signal, which represents the total light power hitting the detector. The second is the difference signal which is proportional to the position of the light on the detector multiplied by the total power. As inputs, the amplifier receives (1) the current from the lateral cell, (2) two gain control bits to select one of four gains for the difference signal, (3) an offset signal which effectively adjusts the center point of the detector when operating in DC coupled mode, and (4) ± 15 V power.

Note that since the difference amplifier gain and offset must be adjusted while the detector is rotating and the cone is being centered, they are controlled by signals which pass through the slip ring assembly. The gain adjustments for the detector preamplifiers located on the rotating PC board need only be adjusted if the total power on the lateral changes significantly.

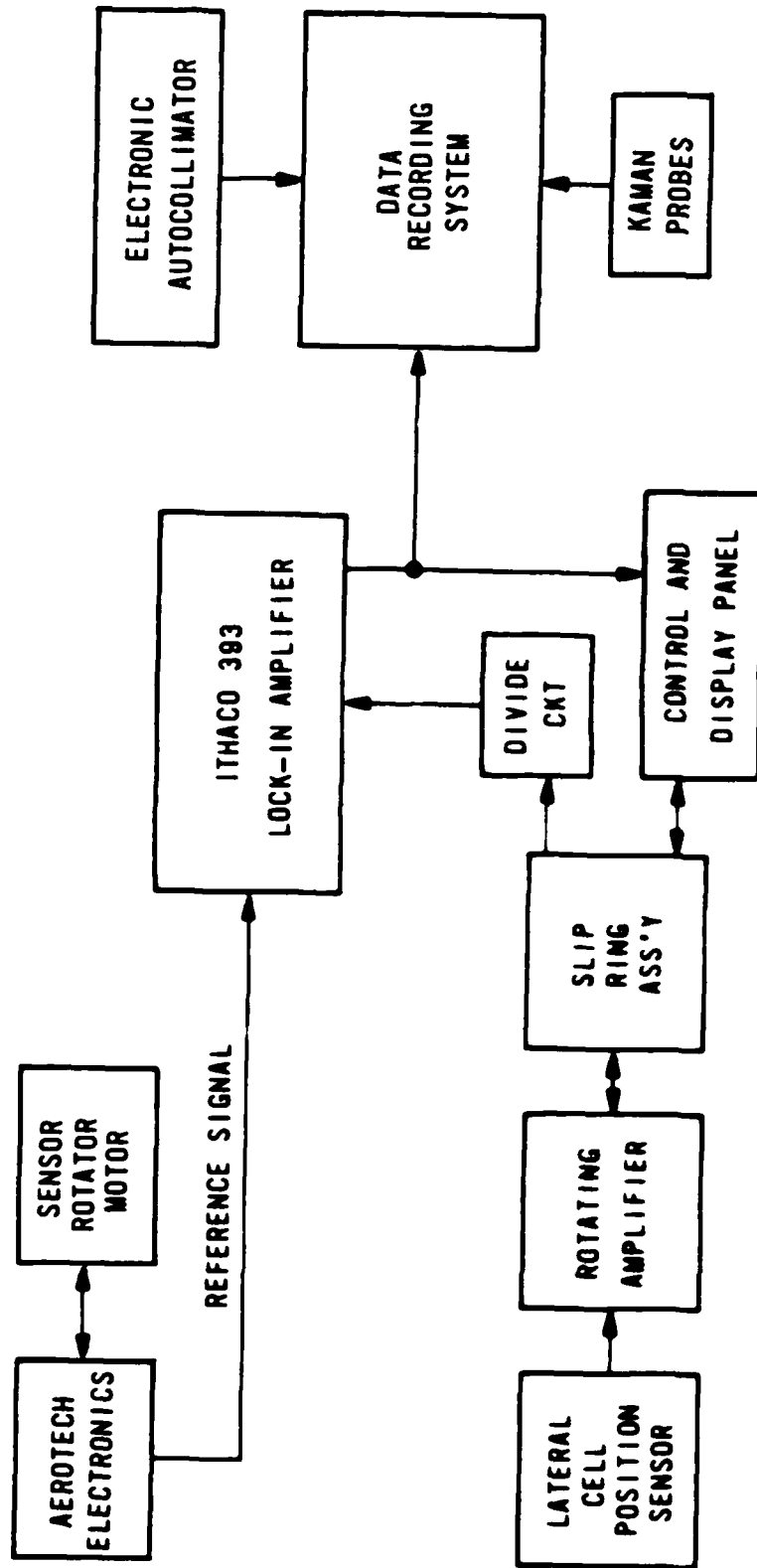


Figure 1' Block diagram of electronics.



Figure 16. Lock-in detector amplifier.

3. DIVIDE CIRCUIT

The divide circuit divides the two channels of the detector amplifier: the difference signal from the lateral cell detector and the total power signal required to produce the beam's position along the detector's sensitive axis and to compensate for variations in the amount of light hitting the detector. The circuitry consists of an Analog Devices Model 4368 two-quadrant analog divider hybrid integrated circuit plus the associated trim potentiometers. The circuit has a 0.10 percent (of full scale) accuracy specification provided the denominator voltage is between 0.1 and 10 V.

4. LOCK-IN AMPLIFIER

The lock-in amplifier (Fig. 15) combines the angle of the rotating detector with the position of the light on that detector to produce X-axis and Y-axis cone centration errors. An Ithaco Model 393 lock-in amplifier was used in its external mode with optional low frequency (brown) cards to permit operation on signals down to 0.1 Hz.

The fundamental frequency of the position of the light on the detector is the same as the frequency of the detector's rotation. The lock-in amplifier, in effect, filters the noise out of the detector signal to leave only the fundamental frequency, then computes the amplitude, A , and the phase angle, ϕ . It outputs $A \cos \phi$ and $A \sin \phi$, which are the cone and centration errors in the X and Y axes, respectively.

Figure 17 shows a sample of the position detector signal that is sent to the lock-in for the rather large decentration of 1.3 mm. The plot spans approximately 1.9 revolutions of the detector. The waveform is approximately a sine wave, and repeats itself exactly for each revolution of the detector.

Figure 18 shows nine different position detector signal waveforms for the centered cone and eight different small decentrations about the center. Note that even in the center waveform, where the cone is centered, a significant amount of beam position variation exists. This variation has a fundamental frequency exactly three times the rotation frequency of the detector spindle, and repeats itself exactly each revolution. The source of this third harmonic of the rotation frequency has not been determined. The lock-in amplifier successfully filtered out all but the fundamental frequency to give an accurate reading of decentration.

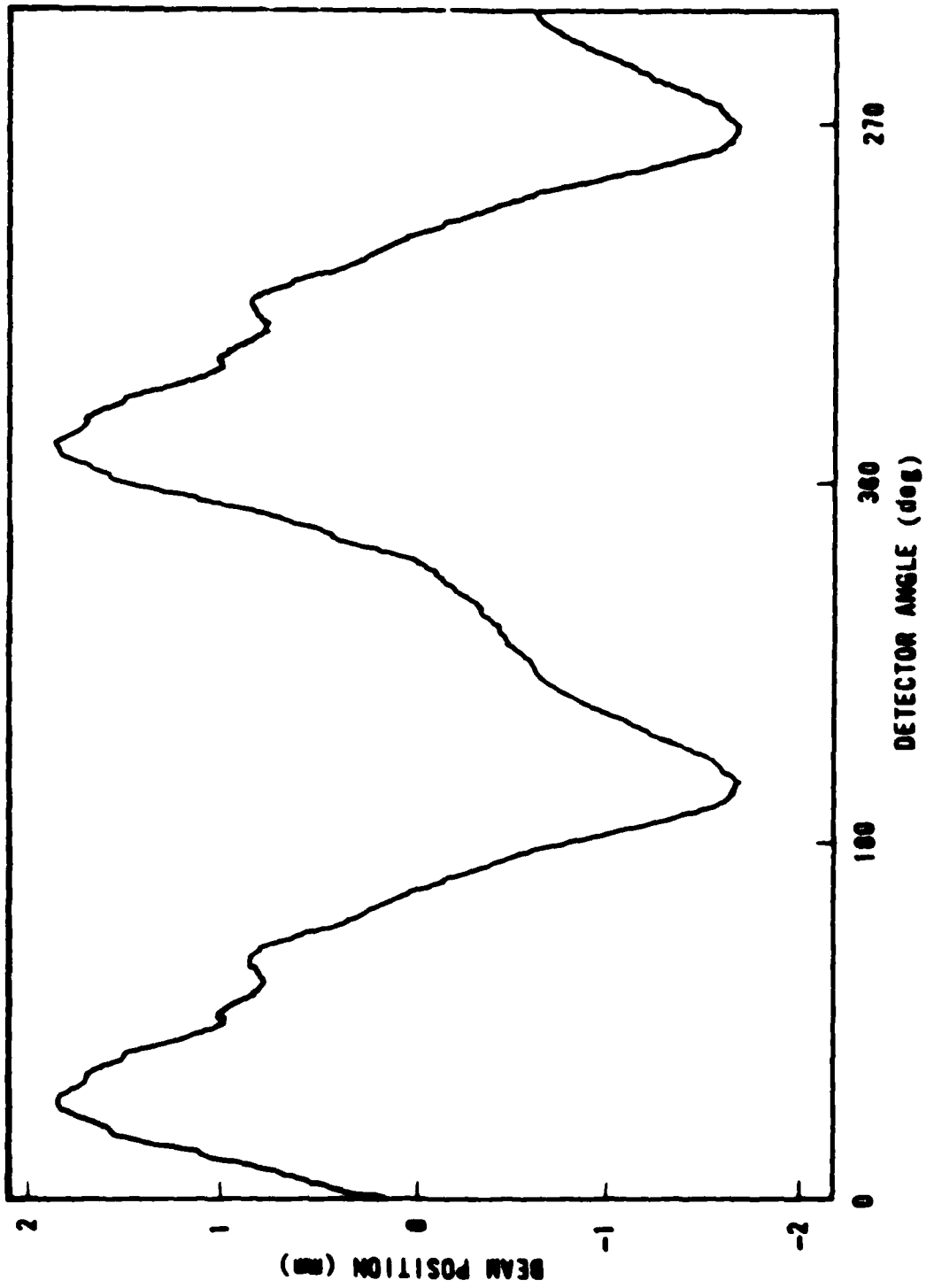


Figure 17. Position detector signal.

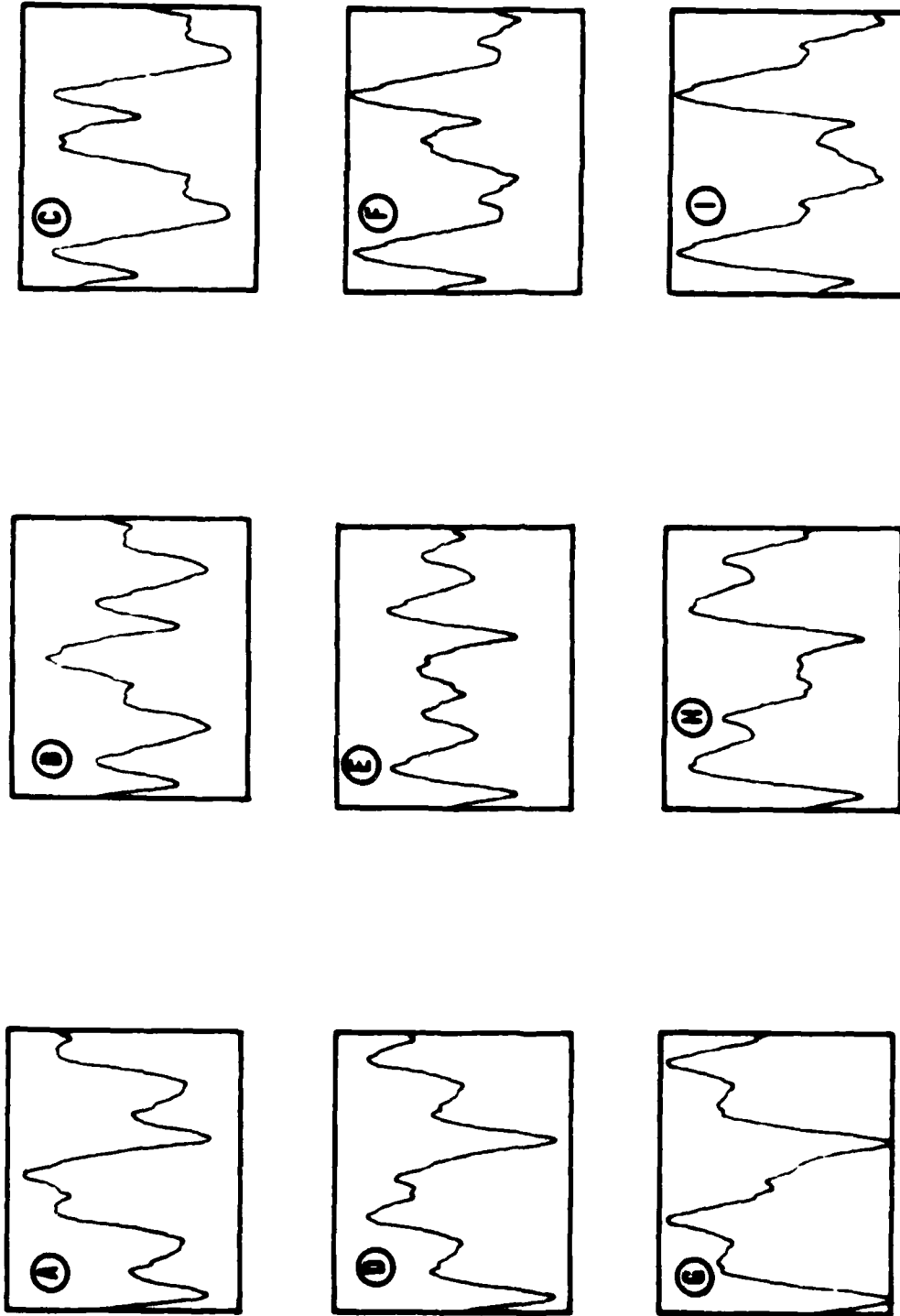


Figure 18. Beam position versus detector angle for various cone decentrations. Vertical axis for all plots is 2.2 mm full scale. Horizontal axis is 560° full scale. Decentrations (X,Y) in mm are: A. (-0.5, 0.5), B. (0, 0.5), C. (0.5, 0.5), D. (-0.5, 0), E. (0, 0), F. (0.5, 0), G. (-0.5, -0.5), H. (0, -0.5), I. (0.5, -0.5).

Applicable performance specifications of the Ithaco 393 lock-in amplifier are summarized below:

Harmonic Rejection: 55 DB
 Bandpass Filter Q: 100
 Accuracy: ±1%
 Linearity: 0.05%
 Frequency Range: 0.1 to 20 Hz

5. CONTROL AND DISPLAY PANEL

The control and display panel displays the cone centration error on two zero center analog meters, and displays beam position, power, normalized position, and output to lock-in amplifier on a third meter. It also contains the position offset control and sensor amplifier gain selector. The panel meters are lighted so that the system may be operated in dim light. The system is housed in a 19 inch rack mount chassis along with the divide circuit and power supply.

6. THE DETECTOR

A Silicon Detector Corporation Model SD-1166-21-11-391 single axis lateral cell position detector (Fig. 12) was used as the detector. This detector measures the centroid along one axis of the light hitting it. Applicable specifications are:

Guaranteed position measurement
 accuracy over operating range: ±0.06 cm

Minimum detectable position
 change (where P = total power
 in watts and f = bandwidth in Hz): $10^{-3} \sqrt{f/P} \text{ \AA}$

Measurement range: -1.48 to +1.48 cm

Maximum total light power or
 device at 0.6328 μm: 0.4 mW

Maximum intensity at 0.6328 μm: 200 mW/cm²

VI. ALIGNMENT OF OPTICS

This section describes the procedures used to align the optics.

1. OVERALL ALIGNMENT

The angular alignment of the cone, waxicon, laser lens, and flats was performed using Davidson Model D-275 alignment telescopes which have an accuracy of 25 μ rad. The angles of the waxicon and cone were aligned by autocollimating off of a plate of glass held against their front surfaces. Interferometric alignment was used to make the two lasers beams colinear. Standard procedures were used, and will not be described here (Ref. 3).

The laser was centered on the waxicon by using the centration sensor to minimize power fluctuations rather than beam position fluctuations. Initial cone centration was accomplished to within 1 mm using the interferometer arrangement shown in Figure 4 with the reference mirror covered. Figure 5 shows the output beams observed with the cone centered, (a), decentered by 1 mm, (b), decentered by 2 mm, (c), and decentered by 4 mm, (d). Dark spots 1 and 3 on Figure 5 are both caused by a single small pit on the inner part of the waxicon. Dark spot 2 is caused by rounding of the central tip of the waxicon.

2. ROTATING SENSOR TO CONE ALIGNMENT

The axis of rotation of the detector rotator spindle must be aligned so that it is perpendicular to the axis of the cone, and the detector must be aligned so that its axis of rotation passes through its active surface. The angular alignment was performed by means of a one inch mirror (Fig. 11) at the end of the spindle. This mirror was adjusted for the least possible amount of motion using an autocollimator while the sensor rotated. The residual motion, caused by wobble in the bearings, was 70 μ rad 0-P (zero to peak). Decentering of the sensor mount with respect to its axis of rotation, measured with a mechanical dial indicator, was found to be less than 25 μ m. This mirror, now perpendicular to its axis of rotation, was then aligned to the reference surface of the cone by autocollimating off of a plate of glass held against the front of the cone. An accuracy of 1 mrad was achieved.

3. German, J. D., "Practical Considerations in the Alignment of Annular Resonators," Laser Digest--Fall 1980, AFWL-TR-81-9, Air Force Weapons Laboratory, Kirtland Air Force Base, NM (1981).

The active surface of the lateral cell detector was centered on the axis of rotation (Fig. 12) using a micrometer according to the specification that the active surface be 0.090 inches from the top surface of the lateral cell. Using this procedure, the distance from the axis of rotation was reduced to within 1 mm and the angular misalignment was reduced to less than 1.0 mrad. This made the total contribution to cone centration error an insignificant 1.0 μm .

3. LENS TO WAXICON TIP ALIGNMENT

The lens was centered in its rotating mount (Fig. 10) by illuminating the lens with collimated light and observing the image motion in its focal plane with a microscope. Centration to 17 μm was achieved. Centration of the reticle was performed in a similar manner by observing the movement of the reticle with a microscope as the reticle lens assembly was rotated. An accuracy of 10 μm was achieved. In both cases, the centering accuracy was limited by the accuracy of the rotation bearings. The reticle was aligned to the waxicon tip with an autocollimating alignment telescope.

VII. EFFECT OF MISALIGNMENTS ON CENTRATION SENSOR ACCURACY

This section describes the effects of optical misalignments on centration sensor systems performance.

1. LASER ALIGNMENT

The most sensitive alignment in terms of centration sensing is the alignment of the angle of the light from the beam expander. The effect on the indicated centration, ΔX , is

$$\Delta X = r\phi$$

where r is the distance from the beam expander to the detector and ϕ is the misalignment of the light from the beam expander. Since r is quite large, 3.5 m, each 1 μ rad error in this beam will cause 3.5 μ m of centration sensor error. In this experiment, the angle of this beam was used to define the optical axis, and therefore, was not counted in the total error. However, the angular drift of the laser was counted and is described in Section VIII-2.

A 2 mm or less decentration of the laser beam has no effect on the indicated centration because the centration sensor system measures centration with respect to the center of the lens, rather than the center of the laser beam. As the beam diameter at the tip of the waxicon is only 11 mm, larger decentration of the laser beam will cause the intensity on one side of the annular beam to be much greater than on the other. This will produce two types of errors. First, the divide circuit will attempt to divide by a voltage outside its range.

Second, the variation in the intensity of the beam over the width of the detector will cause the centroid (Fig. 19), which the detector measures, to be slightly different from the geometric center (which should be measured). As the cone becomes centered, the centroid (intensity center) will coincide with the geometric center and this error will diminish since the intensity pattern on the detector will no longer vary with the detector angle. Swain (Ref. 2) has estimated this error to be a maximum of 23 μ m for a 10 percent azimuthal intensity.

2. WAXICON ALIGNMENT

A small decentration of the waxicon is equivalent to an equal decentration of the cone. This was confirmed in the laboratory. Decentrations of

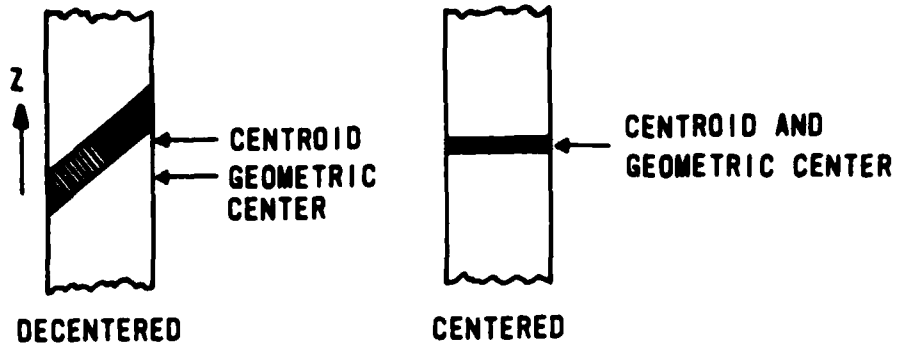


Figure 19. Intensity patterns on the detector.

more than 2 mm will cause divide circuit errors as described in paragraph VII-1.

Angular misalignment of the waxicon produces an effect similar to angular misalignment of the cone. Each 1 μm of misalignment of the waxicon was observed to change the centration sensor system's indication by 0.056 μm .

3. LENS ALIGNMENT

Decentration of the lens produces a centration sensor system signal equivalent to an equal decentration of the cone. This is because the center of the lens defines the optical axis of the system. The collimated light from the laser focuses at a point directly behind the center of the lens. This was confirmed in the laboratory.

Angular misalignment of the lens has only a small effect on the centration sensor system's reading. Aberrations caused by lens tilt have little effect on the centration sensor system since the lateral cell position detector measures the true centroid of the beam. The dominant effects are movement of the laser beam as it passes through the tilted lens and lens translation caused by the lens mount. Each 1 μrad of lens tilt was observed to produce 0.025 μm of change in the indicated centration.

4. SPIDER MIRROR ALIGNMENT

Misalignment of the spider mirror affects the centration sensor system reading directly because the spider mirror alignment contributes to the definition of the optical axis of the resonator. Angular misalignment produces an error, ΔX , in the indicated centration of

$$\Delta X = 2r\theta$$

where $r = 1.45$ m is the optical path length from the spider mirror to the detector and θ is the misalignment of the spider mirror.

5. SENSOR ALIGNMENT

Misalignment of the rotating detector will produce an error, ΔX , in the indicated centration of

$$\Delta X = \theta d$$

where d is the distance from the detector surface to the detector spindle's axis of rotation and θ is the angle between the detector surface and the detector spindle's axis of rotation. The centration of the detector assembly with respect to the center of the cone has very little effect because all of the light reaching the detector from the cone is perpendicular to the active surface of the detector (Fig. 3).

VIII. ERROR SOURCES

The sources of centration error which produced significant errors in this experiment, or which could produce significant errors are described in this section. The magnitude of these errors could not be measured directly because a more accurate alignment system does not exist. These error sources are divided into two categories: (1) static errors--those which do not vary with time, and (2) dynamic errors--those which do vary with time.

1. STATIC ERROR

The sources of static error described below amount to 33 μm when root sum squared (RSS) together.

a. Reticle to waxicon tip alignment. Alignment of the reticle to the waxicon tip was within 26 μm , thus contributing 26 μm to the total centration error. This figure was calculated by multiplying the 25 μrad alignment telescope accuracy by the 1.04 m lens to waxicon tip distance. When using a reflexicon instead of a waxicon, the lens can be placed closer to the tip, making this error correspondingly smaller.

b. Lens to reticle misalignment. Alignment of the center of the lens to the reticle was performed, as described in Section VI-3, to within 20 μm . The limiting factor in this alignment was the slightly irregular motion in the lens bearings. This misalignment contributed 20 μm to the total centration sensor error.

2. DYNAMIC ERROR

The 40 μm peak of dynamic error are illustrated in Figure 20. These changes in indicated centration occurred over approximately 1,000 seconds during which no changes were made in optical alignment. Although Figure 20 shows only about 10 μm (peak) of drift, up to 40 μm of drift were observed over longer periods of time. The high frequency modulation on the two curves is the rotation frequency of the sensor, 0.2 Hz. The source of the lower frequency variations in Figure 20 has not been positively identified, but it appears to be caused by variations in output angle of the laser beam.

a. Drift from the laser. The 40 μm peak drift illustrated in Figure 20, is most likely due to angular drift of the light from the centration laser

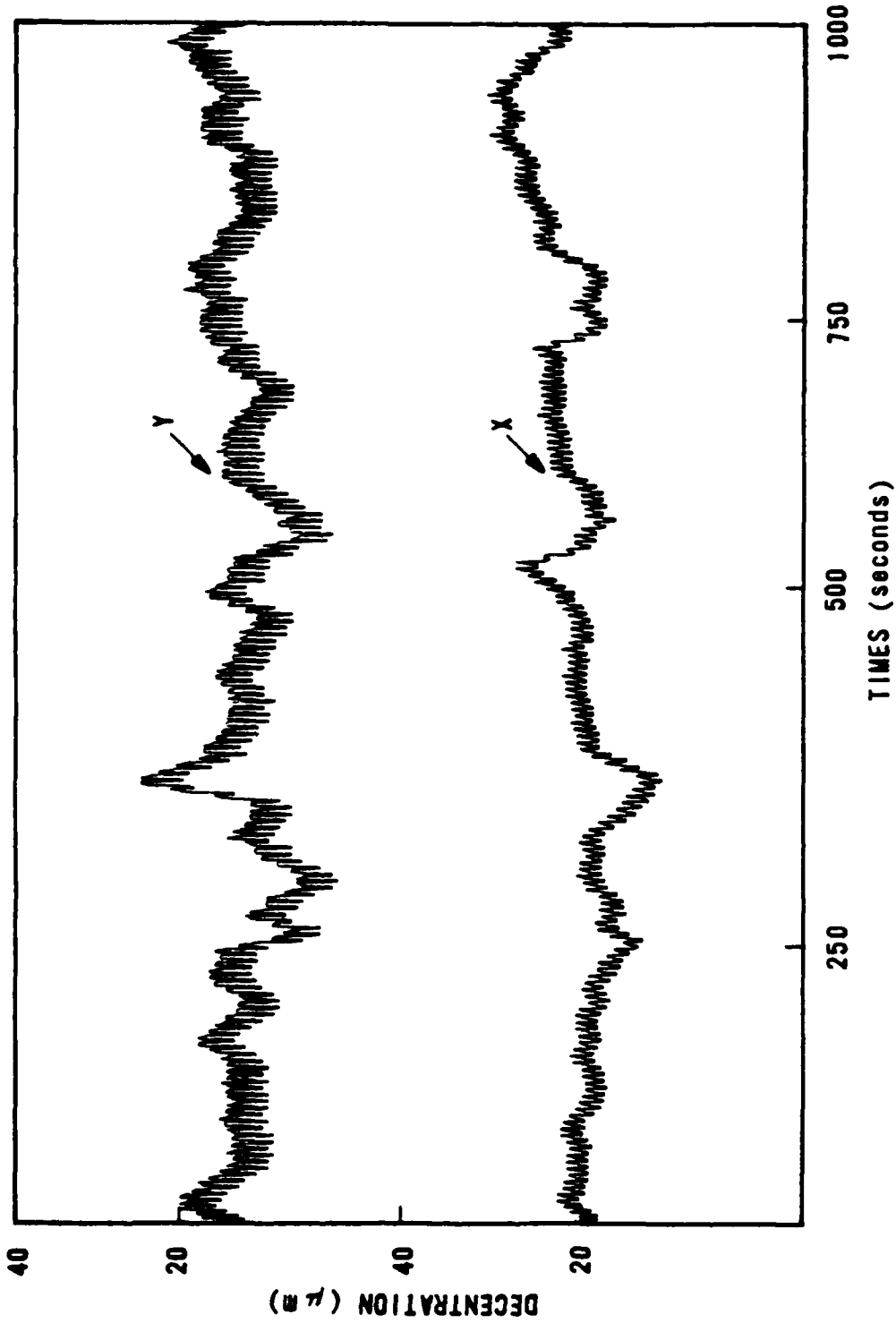


Figure 20. Centration sensor drift.

and beam expander. This affects the centration reading, ΔX , according to the equation

$$\Delta X = R\theta/M$$

where R is the distance from the laser to the detector, 3.5 m, θ is the angular drift of the laser light, and M is the magnification of the beam expander. Thus, a mere 5 μ rad drift in laser output causes a 18 μ m deviation in centration indication. No angular drift specification was available from the laser's manufacturer, and the actual drift after warmup was not measured. However, the drift of the light from the beam expander during warmup was measured; it was 0.5 mm at the detector.

b. Misalignments caused by removal and replacement of the sensor.

Changes in the centration after the sensor had been removed and then replaced were so low they were obscured by the 40 μ m drift described above.

c. Other possible sources of error. Certain anticipated sources of error proved to be inconsequential in practice. Atmospheric disturbances did not cause any problems, and so the proposed plexiglass table cover was never used. Noise from the lateral cell position detector, the slip ring assembly, and the electronics proved to be insignificant. Stray light did affect the centration readings, but turning off the fluorescent lights and using the less powerful incandescent lights solved the problem. Optical table vibrations affected the interferometer, but were rejected by the centration sensor system. Vibration from the detector rotator motor also had no effect on performance.

IX. TEST RESULTS

1. PERFORMANCE

The overall accuracy of the centration sensor system was 52 μm . The sensitivity of the centration sensor system was limited to 40 μm because of low frequency variations in indicated centration, described in Section VIII-2a. The linearity and orthogonality of the centration sensor were better than 1 percent. The lock-in amplifier locked in within 2 min or less. The lock-in amplifier output was stable within 12 s after each adjustment of the optics. Once the system was initially put into operation, it functioned flawlessly throughout 4 mo of testing.

2. PERFORMANCE OF THE SIMPLIFIED SYSTEM

In tests performed to estimate the performance of the centration, the lock-in amplifier remained in operation, but its outputs were hidden from the operator. The cone was decentered up to 2 mm in a random direction, then the operator attempted to center the cone using an oscilloscope display (Fig. 18) of the laser beam position versus detector angle. After the operator had centered the cone to his own satisfaction, the decentration as determined by the lock-in amplifier and the time required to achieve that centration were recorded.

Results of the test with Mr. C. R. DeHainaut as operator are shown in Table 1. The author could center the cone to within about 250 μm (RSS) without benefit of the lock-in amplifier. The test was repeated with Ms. Eleanor L. Coates who was not as familiar with the system at that time as Mr. DeHainaut. After seven trials, she could center the system just as quickly as Mr. DeHainaut, but only to within 500 μm .

TABLE 1. MANUAL TRIALS

Trial	Centration				Time to Center (s)	Day of Test
	X μm	Y μm	θ ($^\circ$)	R (μm)		
1	-106	317	108	334	509	12/4
2	-89	10	174	90	456	12/4
3	7	300	89	300	208	12/4
4	-20	17	140	26	164	12/4
5	99	-43	-23	108	274	12/12
6	92	-251	-70	267	277	12/12
7	59	-168	-68	182	214	12/12
8	56	-106	-62	120	216	12/12

X. CONCLUSION

A cone centration sensor system has been designed, analyzed, built, and tested. Analysis has shown that if the cone is angularly aligned to the optical axis of the resonator, the centration sensor system will indicate when the cone is exactly centered on the optical axis. The centration sensor system is insensitive to cone tilt.

Tests showed that the centration sensor system indicated cone centration to within 52 μ m. This is roughly three times the accuracy required and five times the accuracy achievable without use of the lock-in amplifier. The error sources were identified and quantified so that a more accurate system could be built if desired.

END

DATE

FILMED

11-81

DTIC